

# Methodology for testing an aircraft with cycloidal propulsors in a wind tunnel

*Dmitrii Dekterev*<sup>1,2\*</sup>, *Konstantin Finnikov*<sup>1,2</sup>, *Artem Dekterev*<sup>1,2</sup>, *Andrey Sentyabov*<sup>1,2</sup> and *Aleksandr Dekterev*<sup>1,2</sup>

<sup>1</sup>Institute of Thermophysics SB RAS, 630090, Lavrent'eva ave.1, Novosibirsk, Russia

<sup>2</sup>Siberian federal university, 660074, Svobodny ave. 79, Krasnoyarsk, Russia

**Abstract.** The article describes a technique that makes possible to compile a minimum required program for testing an aircraft with cycloidal propulsors in a wind tunnel to find a given flight mode. By flight mode we mean a mode in which the lift force corresponds to the mass of the aircraft, the thrust compensates for the drag that occurs at a given speed of the oncoming flow, and the pitch, yaw and roll torques are insignificantly small. An analytical model is described that uses experimental data and CFD modeling to find the flight mode and the iterative steps necessary to determine the correction factors. The use of the described method allowed us to demonstrate the flight modes of the aircraft at speeds of 10, 15 and 20 m/s during wind tunnel tests.

## 1 Introduction

When creating new aircraft, a fundamentally important task is confirmation of declared flight characteristics. Conducting of direct flight tests is the final stage in the process of development, debugging and testing of elements and the aircraft as a whole.

The intermediate stages include: laboratory, bench, ground and tethered tests. The most valuable data are the parameters obtained during wind tunnel tests. Due to the uniqueness of large wind tunnels, their small number, workload and the complexity of measurements, wind tunnel tests are a very expensive experiment. The cost of such tests directly depends on the number of standard hours of operation of the wind tunnel.

During the development and testing of an aircraft with cycloidal propulsors [1-3], before conducting wind tunnel tests, the task of minimizing the number of modes required to confirm the declared flight and technical characteristics of the aircraft arose.

To solve the problem, the method of successive approximations was used, implemented in the following order:

1. Using an analytical model, the operating mode of the front and rear rotors is found: pitch angles of blades and phase angles. The rotation speed is considered to be given.
2. With the founded rotor parameters, the cyclocopter is tested in a wind tunnel and the vectors of force and torque acting on it are determined. In addition to the founded mode, 16

---

\* Corresponding author: [dektev\\_da@mail.ru](mailto:dektev_da@mail.ru)

more modes constructed by successively changing the blades pitch angles and phase angles of the front and rear rotors by  $\pm\Delta$ , so that a so-called point cloud in the form of a cube is formed around the desired mode are tested. The desired optimal mode is obviously located inside the cube.

3. Using the measured force and torque vectors, the analytical model of the aircraft is corrected and the entire process is repeated starting from step 1, with reducing of the  $\pm\Delta$  value for cube formation.

During the tests, it was necessary to carry out 3 to 4 repetitions of the described cycle to achieve the desired balance of forces and torques with an acceptable error.

The analytical model of the cyclocopter was based on analytical dependencies of the forces and torques acting on each of the rotors  $F, T(\varepsilon, \phi, V/(\omega R))$ , where  $\varepsilon$  – blades pitch angles,  $\phi$  – phase angles,  $V$  – oncoming flow velocity,  $\omega R$  – rotor circumferential speed. These analytical dependencies were constructed based on measurements of the forces and torques acting on the rotor under oncoming stream conditions in a wind tunnel. Correcting factors were introduced into the analytical dependencies – a scaling factor and an additional angle of rotation of the force vector – determined by comparing the original analytical model with the results of three-dimensional numerical modeling of the aircraft. The need for correcting factors is associated with the mutual influence of the flows created by the oncoming stream, rotors and fuselage. In addition, the forces and torques acting on the fuselage of the vehicle were determined from the modeling results. The correction of the analytical model in paragraph 3 of the above-described method of successive approximations consisted of adding additional terms to the total force and torque, such that the calculated values of the latter were equal to those measured in the previous stage of testing.

## 2 Cycloidal rotor and aircraft assembly

The operating mode of the cycloidal rotor (Fig. 1) is set by three parameters: the rotation frequency, the pitch angle of the blades and the phase angle. The last two parameters are regulated by changing the eccentricity, the magnitude of the eccentricity is responsible for the maximum deviation of the blades from the zero position (pitch angle), and the phase angle of eccentricity of displacement is responsible for the direction of thrust (phase angle).

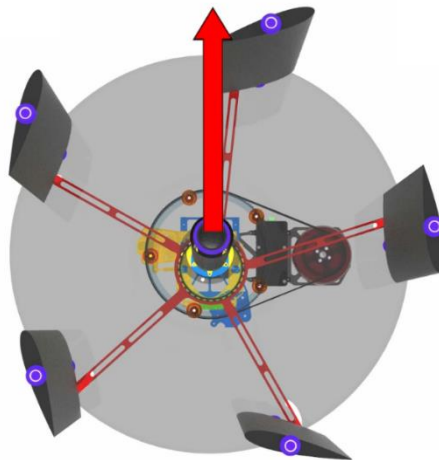


**Fig. 1.** A cycloidal rotor

For an aircraft with four rotors, the number of flight mode parameters becomes equal to 12, which significantly exceeds the number required to ensure the flight mode (in the minimum version, these are three parameters, and when additional conditions of no roll, yaw, and pitch are imposed, six parameters).

The problem is complicated by the fact that in the studied aircraft configuration the front and rear rotors rotate in different directions (fig.2). On the one hand, this leads to more efficient takeoff, landing and hovering modes, due to mutual compensation of overturning torques, on the other hand, it leads to fundamentally different interaction of the front and rear rotors with the oncoming flow. To implement the flight mode, the position of the rotor blades is such that the incident flow imparts additional rotational force attendant with the direction of rotation of the front rotors and counter - for the rear ones. This leads to a significant change in the energy parameters of the rotors, and also contributes to the formation of the direction of thrust and the torques created.

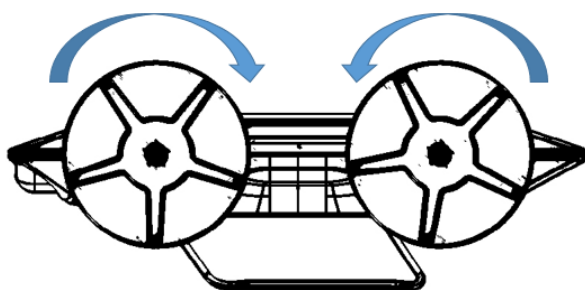


Fig. 2. Aircraft configuration.

### 3 CFD modelling

Based on the data from bench tests of individual propulsors and the assembled aircraft, a numerical simulation of the aerodynamic model of the cyclocopter under flight conditions was performed. The calculation was performed in a three-dimensional formulation, with the  $k-\omega$  SST used as the turbulence model. The sliding mesh method was used for the rotation of the rotors and the movement of the blades. To save computational resources, the computational domain was built for half of the apparatus, and the symmetry condition was applied. The polyhedral computational grid (Fig. 3) consisted of 5.5 million cells. The numerical model was verified using experimental data from a single rotor [4].

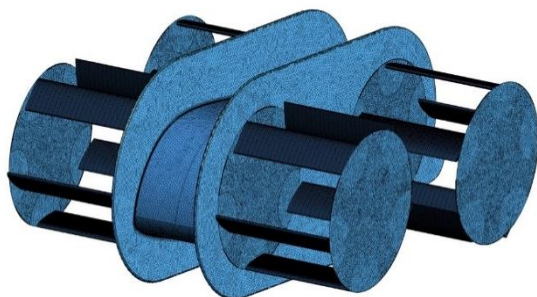
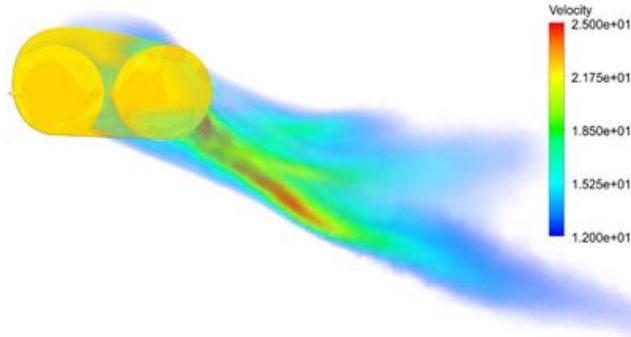


Fig. 3. Computational mesh of the aerodynamic model.

Figure 4 shows the velocity field, which displays the interaction of flows from the front and rear rotors during the flight of the aircraft at a speed of 10 km/h, while the rotation

speed of the rotors is 1100 rpm. The diameter of the rotors is 600 mm with a blade length of 500 mm.



**Fig. 4.** Flow created by an aircraft at a flight speed of 10 km/h.

Figure 5 shows the velocity field, which displays the interaction of flows from the front and rear rotors during the flight of an aircraft at a speed of 20 km/h (rotor speed 1250 rpm).

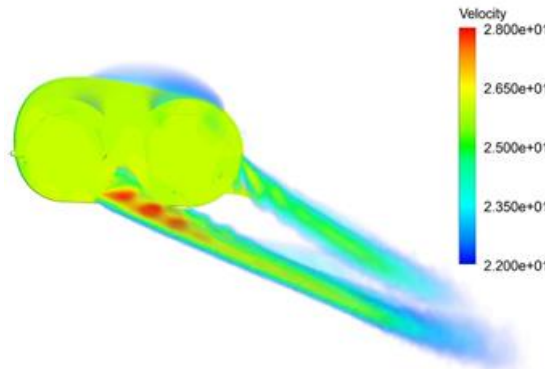


**Fig. 5.** Flow created by an aircraft at a flight speed of 20 km/h.

It is clearly seen that the flows from the front rotors affect the operation of the rear rotors. At the same time, for different flight speeds and different rotor speeds, the flow structure can be significantly rebuilt, which leads to a change in the forces and torques on the rotors and fuselage.

Numerical modeling allows us to estimate the contribution of the oncoming flow to the formation of forces and torques on the front and rear rotors, as well as the fuselage, and is subsequently used to make corrective amendments to the analytical model.

## 4 Analytical model of the rotor

The initial data were the characteristics of the traction and energy parameters of a single cycloidal rotor, obtained during bench tests without incident flow and as a result of wind tunnel tests with flow from 5 to 30 m/s.

When selecting a set of rotor operating mode parameters for constructing analytical dependencies, the following was taken into account:

1. The velocity and pressure fields formed during flow around the rotor at identical values of  $x = V/(\omega R)$ , identical pitch angles and phase angles, are similar, with identical values  $F_{x,y}/\omega^2, T_z/\omega^2$ .

2. The front and rear rotors are geometrically mirror images of each other relative to the plane  $x = 0$ . The reflection transformation relative to this plane changes the sign of the velocity, phase angle,  $F_x, T_z$  and leaves  $F_y$  and the absolute value of the angular velocity of the rotor unchanged (it is this, and not the value of the projection of the angular velocity vector onto the Z axis, that is the working parameter of the rotor).

Therefore,

$$\begin{aligned} -F_x^{front}(-V, -\phi) &= F_x^{rear}(V, \phi); \\ F_y^{front}(-V, -\phi) &= F_y^{rear}(V, \phi); \\ -T_z^{front}(-V, -\phi) &= T_z^{rear}(V, \phi) \end{aligned}$$

On the other hand, transforming the rotation by  $\pi$  radians around the Z axis leaves the rotor modification (front or rear rotor) and the torque unchanged, increases the phase angle by  $\pi$  and changes the signs of the forces:

$$\begin{aligned} -F_x^{front}(-V, \pi + \phi) &= F_x^{front}(V, \phi) \\ -F_y^{front}(-V, \pi + \phi) &= -F_y^{front}(V, \phi) \\ T_z^{front}(-V, \pi + \phi) &= T_z^{front}(V, \phi) \end{aligned}$$

Combining the reflection and rotation transformations, we obtain

$$\begin{aligned} F_x^{rear}(V, \phi) &= F_x^{front}(V, \pi - \phi) \\ F_y^{rear}(V, \phi) &= -F_y^{front}(V, \pi - \phi) \\ T_z^{rear}(V, \phi) &= -T_z^{front}(V, \pi - \phi) \end{aligned} \tag{1}$$

During the calculations, 2 variants of the torques created by the rotor were determined. The first, which we will call the torque and denote as  $T_{zf}$ , is defined as the integral torque of aerodynamic forces on all elements of the rotor. The second torque, which we will call energetic and denote as  $T_{ze}$ , is defined as the torque on the rotor drive shaft. The difference between the above options is due to the fact that the blade repositioning process creates a force on the control sprocket shaft (we emphasize that we are talking specifically about force; the total torque applied to the control sprocket shaft is zero). Due to the displacement of the sprocket shaft relative to the drive shaft, the force on the sprocket shaft creates a torque relative to the drive shaft axis. The rotor torque balance in steady-state operating mode, determined relative to the drive shaft axis, looks like sum of the torque created by the drive, the torque applied to the shaft of the control sprocket, the torque of aerodynamic forces is equal to zero.

As a rule, the energy torque is slightly, by 10-20%, greater than the power torque. This means that part of the torque received by the rotor from the drive is returned to the aircraft structure through the torque applied to the sprocket shaft, and the rest is transferred to the air. When considering the balance of the impulse and the angular momentum of the demonstrator during flight modeling, it is necessary to use the torques on the rotors, since they describe the exchange of the angular momentum between the environment and the rotors. When determining the mechanical power consumed by the rotor, it is necessary to use the energy torque.

The dimensionless forces and torques obtained from CFD modeling and wind tunnel testing are defined as

$$\tilde{F}_{x,y} = \frac{2}{\rho(\omega R)^2 LC} F_{x,y}; \tag{2}$$

$$\tilde{T}_{z f,e} = \frac{2}{\rho(\omega R)^2 RLC} T_{z f,e}.$$

The analytical model of the demonstrator is formulated taking into account the above symmetry relations with respect to rotation by  $\pi$  radians around the Z axis. These relations are satisfied by dependencies of the form

$$F(x, \phi) = \sum_{k=0}^{k_{max}} (f_k(x) \sin(k\phi) + g_k(x) \cos(k\phi))$$

where  $x = V/(\omega R)$ ; functions  $f_k, g_k(x)$  must be even for odd  $k$  and vice versa. For  $T_z$  the form of dependence is similar, but functions  $f_k, g_k(x)$  must be even if  $k$  is even and vice versa. The value of  $k_{max}$  determines the detail of the description of forces and torque from the phase angle. Given the available amount of calculation data, the optimal choice is  $k_{max} = 3$ . The polynomial form of the functions  $f_k(x)$  is chosen: even ones have the form

$$f, g(x) = a + bx^2, a, b = const$$

odd – type

$$f, g(x) = ax + bx^3$$

The CFD data set includes 3 pitch angles - 80%, 90%, 100%, for which calculations with the oncoming flow were performed. With such a necessarily small set of angles, it is advisable to resort to interpolation of the coefficients of the analytical dependence. The case  $x = 0$  can be described in a special way, for which the dependence of forces on the pitch angle is studied in more detail.

The selection of the coefficients of the analytical dependencies was carried out by minimizing the sum of the squares of the differences in the forces determined by the analytical dependence and the forces from the CFD modeling data. In the course of this process, terms were excluded from the analytical dependencies, the presence or absence of which weakly affects the total square of the deviation. The final forms of the dependencies for forces and torques dimensionless in accordance with (2) are as follows:

$$\begin{aligned} \tilde{F}_x(x, \phi) = \tilde{F}_{x0}(\varepsilon)(1 + c_{x0}x^2 + c_{x1}x + c_{x2}x^2 \cos \phi + \\ + c_{x3}x \cos 2\phi + c_{x4}x \sin 2\phi + c_{x5}x^2 \cos 3\phi) \end{aligned} \quad (3)$$

$$\begin{aligned} \tilde{F}_y(x, \phi) = \tilde{F}_{y0}(\varepsilon)(1 + c_{y0}x^2 + c_{y1}x + c_{y2}x \cos 2\phi + \\ + c_{y3}x \sin 2\phi + c_{x4}x^2 \cos 3\phi + c_{x5}x^2 \sin 3\phi) \end{aligned} \quad (4)$$

$$\begin{aligned} \tilde{T}_z(x, \phi) = \tilde{T}_{z0}(\varepsilon)(c_{t0} + c_{t1}x^2 + c_{t2}x \cos \phi + c_{t3}x \sin \phi + c_{t4}x^2 \cos 2\phi + \\ + c_{t5}x^2 \sin 2\phi) \end{aligned} \quad (5)$$

Here  $\varepsilon$  – is the pitch angle normalized to 1. The expressions for  $\tilde{F}_{x0}(\varepsilon), \tilde{F}_{y0}(\varepsilon)$  are derived separately, using the calculated data for  $x = 0$ . This made it possible to describe quite accurately the complex dependence of the thrust angle on the pitch angle in the absence of an incident flow.

The coefficients of dependencies (3, 4, 5) are determined separately for each blade pitch angle. Since the torque is determined in two variants, the set of coefficients for the torque is double. The coefficients used to calculate the power torque are designated as  $c_{tf}$ , for the energy torque –  $c_{te}$ .

Expressions (3), (4), (5) with the specified coefficients are intended for calculating the traction characteristics of the front rotor. The traction characteristics of the rear rotor are calculated using the same expressions with the phase angle and force signs replaced according to (1).

## 5 Application of the analytical rotor model for the implementation of the aircraft flight mode in tests

It is worth considering that the thrust characteristics of the rotor operating as part of the demonstrator differ from the thrust characteristics of a separate rotor. The reason for this is:

- the influence of the fuselage and other rotors on the air flow flowing onto the rotor. This influence is noticeable already in hovering modes without incident flow, with a vertical direction of the rotor thrust vectors.
- the interaction of the rear rotors with the flow disturbance created by the front rotors. This factor becomes significant at high incident flow speeds, when the direction of the air stream created by the front rotor deviates strongly from the vertical backwards. This is aggravated by the fact that high speeds are accompanied by a large phase angle of the front rotor.

The second factor occurs in a limited range of operating modes and should be considered separately. The first is more universal. The differences between the traction characteristics of an individual rotor, calculated using the analytical model, and its actual traction characteristics during operation as part of the demonstrator, are described using rotation and scale transformations:

$$\begin{aligned} F_{xd} &= S(F_x \cos \theta - F_y \sin \theta) \\ F_{yd} &= S(F_y \cos \theta + F_x \sin \theta) \\ T_{zd} &= S_t T_z \end{aligned} \tag{6}$$

$F_{x,y}, T_z$  – traction characteristics of an individual rotor calculated using an analytical model,  $F_{xd,yd}, T_{zd}$  – real characteristics as part of the demonstrator,  $S, S_t$  – scaling factors for force and torque,  $\theta$  – angle of rotation. Scaling factors and rotation angles differ for front and rear rotors.

The next addition to the aircraft flight model is the consideration of the forces acting on the fuselage. The components of force and torque are determined as a result of CFD modeling of the demonstrator operating modes. After that, based on regression analysis, the ratios for the components of force and torque are obtained:  $F_{hx}, F_{hy}, T_{hy}$ .

Corrective factors  $S, S_t, \theta$  (two sets of these values - for the front and rear pairs of rotors in the demonstrator) can be considered constant only in a limited range of pitch angles and phase angles. In this regard, the search for the demonstrator's flight mode during wind tunnel tests was carried out in an iterative mode. At each iteration, there was a subsequent set of rotor operating mode parameters, which, according to calculations, ensured a balance of forces and torques. For this set and for modes with some shift in pitch angles and phase angles of the front and rear pairs of rotors, the forces and torques acting on the demonstrator in the wind tunnel were measured.

The measurement results were used to determine new values  $S, S_t, \theta$  by searching for the minimum standard deviation of the measured forces and torques from the calculated ones. After this, the rotor operating parameters were determined again, ensuring the balance of forces and torques of the demonstrator, and a new cycle of measuring forces and torques was carried out in the wind tunnel. Rotor speeds were considered as fixed and symmetrical flight modes were considered, in which the operating mode of the right and left rotors in the front and rear pairs is identical. Consequently, the sought parameters were 4 – pitch angles and phase angles of the front and rear pairs of rotors. In the presence of three balance conditions - for  $F_x, F_y$  and  $T_z$  - to determine the sought parameters, the condition of the minimum of the weighted sum of squares of the differences between the rotor operating parameters at a given iteration and at the previous one was additionally adopted. Such a condition was imposed for the purpose of regularizing the iteration process. The iteration process was completed when the balance conditions were met

$$|\sum F_x| \leq 10 \text{ n}, |\sum F_y| \leq 5 \text{ n}, |\sum T_z| \leq 5 \text{ n} \cdot \text{m}$$

In flight modes with pitch and yaw, the Z-component of aerodynamic forces, as well as the X- and Y-components of the torque, arise. In order to obtain the initial data for including this force and torques in the flight model of the demonstrator, CFD modeling of the flow around the demonstrator with pitch and yaw was performed. The rotor operating modes were chosen to be identical to the modes without pitch and yaw, in which closeness



to the balance of forces is achieved. Two variants of such modes were studied: for speeds of 5 and 10 m/s. For the pitch angle, 2 variants were considered:  $+10^\circ$  and  $-10^\circ$ . For the yaw angle, there was 1 variant,  $-10^\circ$  (the mode with a yaw angle of  $+10^\circ$  is its symmetrical reflection along the Z axis).

## 6 Wind tunnel experiment

Ultimately, with the integrated use of bench test data, CFD calculations and an analytical model, a plan for a tube experiment was developed (Fig. 6), which allows, in 3 iterations, to build the operating mode of the aircraft's four rotors in such a way as to compensate for the takeoff weight of the apparatus, the forces of the flow approaching at a given speed and at the same time balance the torques.

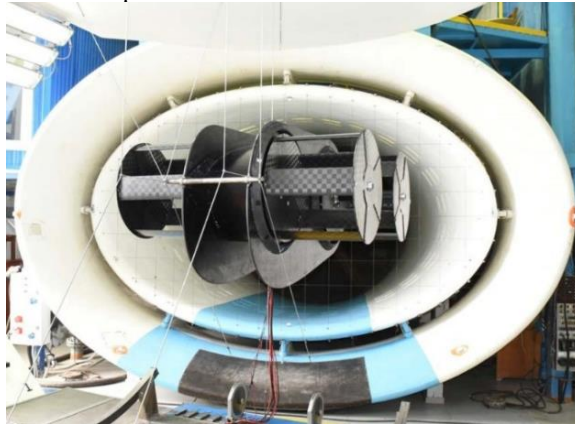


**Fig. 6.** Model of an aircraft with cycloidal propulsors in a wind tunnel

As an example, tabular data are given for finding the flight mode of a 40 kg apparatus, with a rotor speed of 1200 rpm, at a speed of 15 km/h. In the first experiment (table 1), it was necessary to plot 17 points (the first line indicates the mode selected using the analytical model). For the second launch (table 2), 9 points were enough, while the maximum deviation of the variable parameters from the specified point was halved. The third launch (table 3) is a control one, to confirm the desired mode. The following notations are used in the tables:

- $\varepsilon_1$  - Blades pitch angle, front rotors
- $\varepsilon_2$  - Blades pitch angle, rear rotors
- $\phi_{1/2}$  - phase angle, front/rear rotors
- $N$  - Rotor speed

**Table 1.** Rotor parameters for finding the flight mode (step 1)

№	$V$ , m/s	$N$ , rpm	$\varepsilon_1$ , %	$\varepsilon_2$ , %	$\phi_{1/2}$ , °
1	15	1200	88	72	65/69
2	15	1200	78	62	60/64
3	15	1200	78	62	70/74
4	15	1200	78	82	60/64
5	15	1200	78	82	70/74
6	15	1200	98	62	60/64
7	15	1200	98	62	70/74
8	15	1200	98	82	60/64
9	15	1200	98	82	70/74
10	15	1200	78	62	55/59
11	15	1200	78	62	75/79



12	15	1200	78	82	55/59
13	15	1200	78	82	75/79
14	15	1200	98	62	55/59
15	15	1200	98	62	75/79
16	15	1200	98	82	55/59
17	15	1200	98	82	75/79

**Table 2.** Rotor parameters for finding the flight mode (step 2)

$N_0$	$V$ , m/s	$N$ , rpm	$\epsilon_1$ , %	$\epsilon_2$ , %	$\phi_{1/2}$ , °
1	15	1200	77	63	60/75
2	15	1200	72	58	55/70
3	15	1200	72	58	65/80
4	15	1200	72	68	55/70
5	15	1200	72	68	65/80
6	15	1200	82	58	55/70
7	15	1200	82	58	65/80
8	15	1200	82	68	55/70
9	15	1200	82	68	65/80

**Table 3.** Rotor parameters for flight mode confirmation

$N_0$	$V$ , m/s	$N$ , rpm	$\epsilon_1$ , %	$\epsilon_2$ , %	$\phi_{1/2}$ , °
1	15	1200	76	64	62/63

Similar experiments were conducted for different rotor speeds and incident flow velocities from 10 to 30 m/s. It is noted that for flow velocities of 10 m/s and below, the phase angles for the front and rear rotors can have the same values.

## 7 Conclusions

Traditional approaches to the study of aircraft flight modes in wind tunnels require a long-term experiment with systematic changes in a number of parameters and the acquisition of a huge array of data and their subsequent processing. The presented methodology is an iterative process based on a preliminary comprehensive analysis of experimental data, numerical modeling data and an analytical description of the aircraft operation. This allows for a significant reduction in the number of modes being studied and accordingly minimize the standard operating hours of the wind tunnel, which is more economically advantageous. At the same time, the stated flight characteristics are accurately confirmed.

The use of the described method allowed us to demonstrate the possibility of flight of the aircraft with cycloidal propulsors with a takeoff mass of more than 40 kg during tests in the T-203 SibNIA wind tunnel. Parameters for stable horizontal flight of the aircraft at speeds of 10, 15 and 20 m/s were obtained.

## 8 Acknowledgements

The study was carried out under state contract with IT SB RAS (124062400029-2).

## References

1. C.M. Xisto, J.C. Prascoa, J.A. Leger, P. Masarati, G. Quaranta, M. Morandini, L. Gagnon, D. Wills, M. Schwaiger, Numerical modelling of geometrical effects in the performance of a cycloidal rotor, in Proceedings of 11th World Conference on Computational Mechanics, Barcelona, Spain (2014), T. 1252.

2. M. Benedict, M. Ramasamy, I. Chopra, Improving the aerodynamic performance of micro-air-vehicle-scale cycloidal rotor: An experimental approach. *J. Aircraft.* **47**, 1117-25 (2010).
3. G. Iosilevskii, Y. Levy, Experimental and numerical study of cyclogiro aerodynamics. *AIAA J.* **44**, 2866-70 (2006).
4. Ar. Dekterev, A. Dekterev, D. Dekterev, Y. Goryunov, Investigation of the effects of end faces design on parameters of cycloidal rotor. *Journal of Physics: Conference Series.* **1105(1)**, 012029 (2018).